An Efficient Sub-Cycle Alternative to Instantaneous Power Metrics

Afsaneh Ghanavati, Hanoch Lev-Ari and Aleksandar M. Stanković

Abstract-In this paper we discuss the relationship between sub-cycle and instantaneous power metrics in polyphase AC systems. While both approaches have very low computational cost, which makes them suitable for real-time control of industrial processes, the 2-sample sub-cycle scheme offers several distinct advantages over the purely-instantaneous approach. In particular, we show that: (a) the level of steady-state fluctuation of subcycle power metrics that use only two time-domain samples is significantly lower than that of purely-instantaneous metrics, and (b) the sub-cycle scheme generates several additional power metrics, which can be used to detect onset of faults, and accurately determine their duration. We illustrate our points using both synthetic and (real-life) industrial examples. In addition, we examine the connection between the 2-sample sub-cycle scheme and other near-instantaneous approaches, based on derivatives of currents and voltages. We again observe a significantly lower numerical sensitivities for the 2-sample sub-cycle quantities. Furthermore, 2-sample quantities have a unique feature that they can naturally be extended to more samples, with concomitant reduction in fluctuations, better accuracy and with only moderate increase in computational cost. We posit that the sub-cycle approach has promise in detection, control and classification applications.

Keywords—instantaneous power metrics, dynamic phasors, dynamic sub-cycle power metrics, derivative-based reactive power, power system transients, fault detection.

I. INTRODUCTION

Electric energy systems have been undergoing profound changes, as new technologies have entered their major domains – distributed generation with renewable sources, voltage-sourced HVDC in transmission, power electronic converters in distribution, feedback-controlled loads, and new aggregates such as microgrids. These new components and entities are invariably connected with more frequent variations in system structure and parameters, thus increasing the importance of characterization and quantification of system transients. Among most important and widely used quantities for both engineering and economics are power quality measures.

A. Ghanavati (ghanavatia@wit.edu) is with the Electrical and Computer Engineering Program, School of Engineering, Wentworth Institute of Technology, Boston, MA 02115. H. Lev-Ari (levari@ece.neu.edu) is with the Department of Electrical and Computer Engineering, Northeastern University, Boston, MA 02115. A.M. Stanković (astankov@ece.tufts.edu) is with the Department of Electrical and Computer Engineering, Tufts University, Medford, MA 02155. This work was supported in part by ONR grants N00014-10-1-0538 and N00014-16-1-3028, by NSF under grant ECCS-1710944, by the NSF/DOE Engineering Research Center Program under NSF Award EEC-1041877, and by the CURENT Industry Partnership Program.

The role of monitoring, control, analytics and forensics in power systems has always been a very important one. In addition, the increase of power-electronics interfaced components such as renewable sources, electric vehicles and controllable loads has resulted in the need for high-resolution monitoring technology, extensive data-logging, and versatile decision support for network-wide diagnosis and control. For example, the rise of wide-area and model-based protection algorithms necessitates a very accurate detection of the onset of a transient so that appropriate protection algorithms can be initiated [1]. A variety of industrial informatics tools and techniques have been deployed on the problem of event detection in the physical and cyber layers of energy systems [2]–[5].

The overall control capability has also grown in electric energy systems, as power electronic components have enabled increase in control bandwidths. Together with better communications, this grand convergence of technologies resulted in foundations of cyber-physical power systems. This emerging emphasis on speed and precision of the controlled system response has brought to the forefront the need to develop fast-varying metrics that capture transients well while being relevant for steady-state operation as well.

A key concept here is that of instantaneous reactive power [6], [7] that has been used for functions ranging from protection to control, operation and monitoring. This was a timely, bold and relevant idea, as it initiated much needed discussions about sub-cycle actions (i.e., faster than a period of the AC fundamental). Some generalized or alternative definitions of instantaneous reactive power in polyphase systems with more than three phases were introduced in [8]–[13]. The use of filtering to suppress unwanted high-frequency components of instantaneous reactive power was described in [14]–[17]. Recent applications to the control of power electronic devices were presented in [18]–[20]. The use of instantaneous reactive power for power flow control was proposed in [21]–[25]. A recent comparative survey of instantaneous reactive power concepts is provided in [26].

However, it turns out that the geometry of the unconstrained problem (unbalanced, with harmonics, not exclusively three-phase) is more complicated [10], [11], and requires more information than what can be obtained from a single (vector) sample. A catalog of weaknesses of the original definition of instantaneous reactive power is given in [27]; some causes of difficulties can be gleaned even from a simple dimensionality count – a single-phase sinusoid with known frequency requires two parameters for a full characterization (e.g., magnitude and phase), and the two cannot be unambiguously resolved from a single sample. Another key weakness of the purely-

instantaneous approach is that in the case of general polyphase systems, the definition of instantaneous reactive power is not necessarily unique [10], [11].

In this paper we demonstrate that a significant improvement in the quality of dynamic power metrics, as compared with the purely-instantaneous metrics of [6], can be achieved by using just two time-domain samples of the (polyphase) voltage and current waveforms. The information contained in two samples of any m-phase waveform can be used to construct a dynamic m-phase complex phasor, resulting in a one-toone correspondence between the time and frequency domains. We refer to these phasors as *sub-cycle*, so as to distinguish them from the standard phasors, which require a full-cycle record of the waveform of interest. These (polyphase) phasors are then used to obtain a dynamic decomposition of apparent power, resulting in four distinct sub-cycle power metrics: real power, reactive power, and two additional metrics that characterize distortion power (see [28] and [29] for a detailed exposition). In addition, we can decompose our dynamic ("point-on-wave") real and reactive power metrics into their symmetrical sequence components, which provide additional means to detect and classify transients. It also turns out that the concept we advance in this paper has connections with other near-instantaneous approaches, based on derivatives of currents and voltages, that have been described in papers such as [12], [13], [30].

Fast estimation of the fundamental-harmonic phasor also plays a key role in a number of power-system protection schemes, for example in distance protection of transmission lines. The need for a fast response has motivated the use of fractional-cycle estimation techniques: in particular, phasor estimation from half-cycle data has emerged as a popular choice in protection applications [31, Sec. 2.4], [32]. While our exploration path is aligned with some of these concerns, please note that we are dealing, at each individual time-instant, with a radically smaller number of samples, and thus a significantly reduced computational cost, i.e., 2 samples separated by a quarter-cycle shift, as compared with the 64 adjacent samples used in half-cycle estimation schemes (assuming a typical sampling rate of 128 samples per cycle). Our objective is not the fundamental phasor per se, but rather the construction of almost-instantaneous power metrics, which can be used in control and monitoring of power electronic devices, and also have the potential to support fast detection in protection applications (see Figs. 8 and 11 for an illustration of this capability).

Our dynamic sub-cycle power metrics characterize both steady-state and transient operation of AC systems, based on a small number of voltage and current samples. In particular, the 2-sample sub-cycle scheme, which was first introduced in [33], has essentially the same computational cost as the purely-instantaneous (a.k.a Akagi) approach of [6], [7], and thus can be used in real-time control of industrial processes. However, the 2-sample sub-cycle scheme offers several distinct advantages over the purely-instantaneous approach.

First, notice that the 2-sample sub-cycle approach can be used with any number of phases, including single-phase systems. In contrast, the purely-instantaneous reactive power of [6], [7] is defined only for 3-phase systems. Next, the level of fluctuation caused by higher-frequency components, both in steady-state and in transient operation, is significantly lower for the 2-sample sub-cycle power metrics, as compared with that of the purely-instantaneous real and reactive power. Furthermore, practical applications of the purely-instantaneous reactive power to compensation and active filter control require filtering to suppress the unwanted fluctuating component [14]-[17]: this increases time-delay and phase-lag, resulting in an impaired response to wide-band transients, as well as added implementation cost. In contrast, sub-cycle real and reactive power metrics can be used without further filtering [28], [29]. Finally, the sub-cycle scheme generates several additional power metrics, including the symmetrical sequence components of dynamic real and reactive power, at a modest increase in computational cost. Some of these metrics can be used to detect onset of faults, and accurately determine their duration. The aim of this paper is to demonstrate these features using both synthetic and industrially-relevant examples.

II. DYNAMIC SUB-CYCLE PHASORS

We consider m-phase systems, i.e., systems with m+1 conductors in which the first m are referenced either to a common ground, or to the (m+1)-st ("neutral") conductor. We define the m-dimensional voltage and current row vectors

$$v(t) \stackrel{\triangle}{=} \begin{bmatrix} v_1(t) & v_2(t) & \dots & v_m(t) \end{bmatrix}$$

$$i(t) \stackrel{\triangle}{=} \begin{bmatrix} i_1(t) & i_2(t) & \dots & i_m(t) \end{bmatrix}$$
(1)

where all currents have reference directions "toward" the load (see Fig. 1).

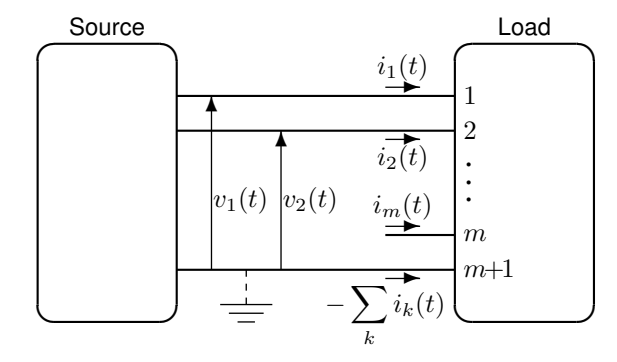


Fig. 1. Circuit schematic of a polyphase system.

The key relation for the sub-cycle approach, as described in [28], [29], is a one-to-one correspondence between *time-domain* waveform samples and *frequency-domain* phasor estimates, given by [29, eqs. (1)-(2)]. In the case of two (polyphase) voltage waveform samples, this relation reduces to

$$\begin{pmatrix} v(t) \\ v(t - \xi T) \end{pmatrix} = \frac{1}{\sqrt{2}} \begin{pmatrix} 1 & 1 \\ e^{-j2\pi\xi} & e^{j2\pi\xi} \end{pmatrix} \begin{pmatrix} \widehat{V}_1(t) e^{j\omega_0 t} \\ \widehat{V}_1^*(t) e^{-j\omega_0 t} \end{pmatrix} (2)$$

and similarly for the current waveform i(t). Here ω_0 is the steady-state fundamental frequency, $T=\frac{2\pi}{\omega_0}$ is the corresponding cycle duration, ξ is a control parameter, and the superscript * indicates element-by-element conjugation (without transposition). Solving this equation for the voltage phasor $\widehat{V}_1(t)$ (and similarly for the current phasor $\widehat{I}_1(t)$), one obtains the explicit expressions

$$\widehat{V}_{1}(t) e^{j\omega_{0}t} = \frac{1}{j\sqrt{2}\sin 2\pi\xi} \left[e^{j2\pi\xi} v(t) - v(t - \xi T) \right]
\widehat{I}_{1}(t) e^{j\omega_{0}t} = \frac{1}{j\sqrt{2}\sin 2\pi\xi} \left[e^{j2\pi\xi} i(t) - i(t - \xi T) \right]$$
(3)

Notice that the sub-cycle phasors $\widehat{V}_1(t)$ and $\widehat{I}_1(t)$ are time-variant row vectors of size $1\times m$: they also provide a *time-frequency representation*, which is not available in the purely-instantaneous approach of [6], [7]. In particular, setting $\xi=\frac{1}{4}$ reduces these expressions to

$$\widehat{V}_{1}(t) e^{j\omega_{0}t} = \frac{1}{\sqrt{2}} \left[v(t) + j v(t - \frac{T}{4}) \right]
\widehat{I}_{1}(t) e^{j\omega_{0}t} = \frac{1}{\sqrt{2}} \left[i(t) + j i(t - \frac{T}{4}) \right]$$
(4)

which require no multiplications (except for scaling by $\frac{1}{\sqrt{2}}$).

In the special case of 3-phase systems (i.e., when $\,m=3)\,$ we can construct the symmetrical sequence components of the voltage and current phasors by applying the unitary transformation

$$\begin{bmatrix} \widehat{V}_{1,0}(t) & \widehat{V}_{1,+}(t) & \widehat{V}_{1,-}(t) \end{bmatrix} \stackrel{\triangle}{=} \widehat{V}_{1}(t) \mathcal{M}_{sc}
\begin{bmatrix} \widehat{I}_{1,0}(t) & \widehat{I}_{1,+}(t) & \widehat{I}_{1,-}(t) \end{bmatrix} \stackrel{\triangle}{=} \widehat{I}_{1}(t) \mathcal{M}_{sc}$$
(5a)

where

$$\mathcal{M}_{sc} = \frac{1}{\sqrt{3}} \begin{pmatrix} 1 & 1 & 1 \\ 1 & \alpha & \alpha^2 \\ 1 & \alpha^2 & \alpha \end{pmatrix} , \quad \alpha \stackrel{\triangle}{=} e^{j2\pi/3} \quad (5b)$$

and the subscripts "0," "+" and "–" denote zero-sequence, positive-sequence and negative-sequence components, respectively. Notice that $\mathcal{M}_{sc}\,\mathcal{M}^H_{sc}=I$, where the superscript H indicates conjugate (i.e., Hermitian) transpose.

III. SUB-CYCLE VS. PURELY-INSTANTANEOUS POWER METRICS

All 2-sample sub-cycle power metrics can be expressed in terms of the voltage phasor $\widehat{V}_1(t)$ and current phasor $\widehat{I}_1(t)$ of (3). In particular, the sub-cycle real and reactive power are determined via the (ξ -dependent) expressions

$$P_{\xi}(t) = \Re\left\{\widehat{V}_{1}(t)\,\widehat{I}_{1}^{H}(t)\right\}\,,\quad Q_{\xi}(t) = \Im\left\{\widehat{V}_{1}(t)\,\widehat{I}_{1}^{H}(t)\right\} \quad \text{(6a)}$$

The sub-cycle apparent power is defined as

$$S_{\xi}(t) \stackrel{\triangle}{=} \|\widehat{V}_1(t)\|_2 \|\widehat{I}_1(t)\|_2 \tag{6b}$$

where $\|\cdot\|_2$ denotes the Euclidean norm of a (complex-valued) vector. The corresponding purely-instantaneous metrics are

 $p(t) = v(t) \, i^\top\!(t), \quad q(t)$ (as defined in [6] via the Clarke transform), and $s(t) = \sqrt{p^2(t) + q^2(t)}$. In this paper, the superscript $^\top$ indicates transposition without conjugation. In general, 2-sample sub-cycle metrics exhibit a significantly lower level of fluctuation in steady-state operation than their purely-instantaneous counterparts.

The difference in the level of steady-state fluctuation is evident, in particular, when the polyphase waveforms v(t) and i(t) are both sinusoidal, namely

$$v(t) = \sqrt{2} \Re \{V_1 e^{j\omega_0 t}\}, \quad i(t) = \sqrt{2} \Re \{I_1 e^{j\omega_0 t}\}$$

In this case we obtain $\widehat{V}_1(t)=V_1$ and $\widehat{I}_1(t)=I_1$, for any choice of ξ , so that $S_{\xi}(t)=\left\|V_1\right\|_2\left\|I_1\right\|_2$, and

$$P_{\xi}(t) = \Re \{V_1 I_1^H\} , \quad Q_{\xi}(t) = \Im \{V_1 I_1^H\}$$

which coincide with the time-invariant results obtained using the standard (i.e., full-cycle) approach. In contrast, the *purely-instantaneous* real power p(t) is time-varying, with a potentially sizable 2-nd harmonic component, viz.,

$$p(t) = v(t) i^{\top}(t) = \Re \{V_1 I_1^H\} + \Re \{V_1 I_1^{\top} e^{2j\omega_0 t}\}$$

Similar results hold for the purely-instantaneous reactive power q(t), which is defined in terms of the Clarke components [6], [7]. Notice that sinusoidal 3-phase voltage and current generate sinusoidal Clarke components, viz.,

$$\begin{array}{lll} v_{\alpha}(t) &=& \sqrt{2}\,\Re\left\{V_{\alpha}e^{j\omega_{0}t}\right\} &, & i_{\alpha}(t) &=& \sqrt{2}\,\Re\left\{I_{\alpha}e^{j\omega_{0}t}\right\} \\ v_{\beta}(t) &=& \sqrt{2}\,\Re\left\{V_{\beta}e^{j\omega_{0}t}\right\} &, & i_{\beta}(t) &=& \sqrt{2}\,\Re\left\{I_{\beta}e^{j\omega_{0}t}\right\} \\ v_{0}(t) &=& \sqrt{2}\,\Re\left\{V_{0}e^{j\omega_{0}t}\right\} &, & i_{0}(t) &=& \sqrt{2}\,\Re\left\{I_{0}e^{j\omega_{0}t}\right\} \end{array}$$

where

$$\begin{bmatrix} V_{\alpha} & V_{\beta} & V_{0} \end{bmatrix} = V_{1} \mathcal{M}_{Clarke}$$
 , $\begin{bmatrix} I_{\alpha} & I_{\beta} & I_{0} \end{bmatrix} = I_{1} \mathcal{M}_{Clarke}$

anc

$$\mathcal{M}_{Clarke} = \frac{1}{\sqrt{3}} \begin{pmatrix} \sqrt{2} & 0 & 1 \\ -\frac{\sqrt{2}}{2} & \sqrt{\frac{3}{2}} & 1 \\ -\frac{\sqrt{2}}{2} & -\sqrt{\frac{3}{2}} & 1 \end{pmatrix}$$

Thus, assuming that zero-sequence components vanish (i.e., $V_0=0=I_0$), the purely-instantaneous reactive power, as defined in [6], is

$$q(t) \stackrel{\triangle}{=} v_{\alpha}(t) i_{\beta}(t) - v_{\beta}(t) i_{\alpha}(t)$$

$$= \Re \left\{ V_{\alpha} I_{\beta}^* - V_{\beta} I_{\alpha}^* \right\} + \Re \left\{ (V_{\alpha} I_{\beta} - V_{\beta} I_{\alpha}) e^{2j\omega_0 t} \right\}$$

We observe that, in this special case, the purely-instantaneous reactive power q(t) also consists of two components (similar to p(t)): (i) a DC (i.e., constant) component, and (ii) a 2nd-harmonic component. The latter vanishes when both the current and voltage are perfectly-balanced.

In order to further illustrate this fundamental difference between 2-sample sub-cycle metrics and purely-instantaneous metrics, consider a synthetic RLC-load example with multiple harmonics (see Sec. A in the Appendix for a detailed

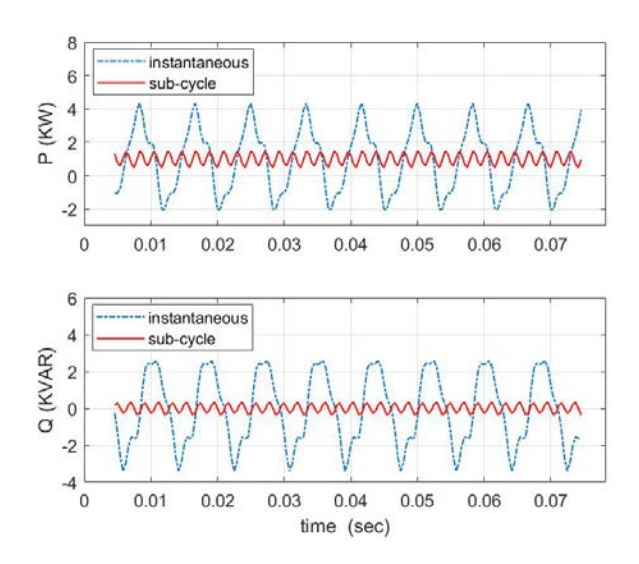


Fig. 2. Synthetic steady-state example (RLC-load): real power (top), and reactive power (bottom). Dash-dot line used for instantaneous metrics, and solid line used for sub-cycle metrics (with $\xi = \frac{1}{4}$).

description). When the source voltage is sinusoidal, the subcycle metrics are constant (and coincide with their full-cycle counterparts), while the purely-instantaneous metrics exhibit a large fluctuating component. Adding a 7-th harmonic voltage component, with amplitude that is 5% of the fundamental, results in further distortion of the instantaneous metrics, but only contributes a mild fluctuating component to the 2-sample sub-cycle $P_{1/4}(t)$ and $Q_{1/4}(t)$ (Fig. 2). The same qualitative difference between 2-sample sub-cycle metrics and purely-instantaneous metrics is also evident in the steady-state-Hydro-Ottawa example (see Sec. B in the Appendix for a detailed description): the purely-instantaneous p(t) and q(t) fluctuate much more than their sub-cycle counterparts (Fig. 3).

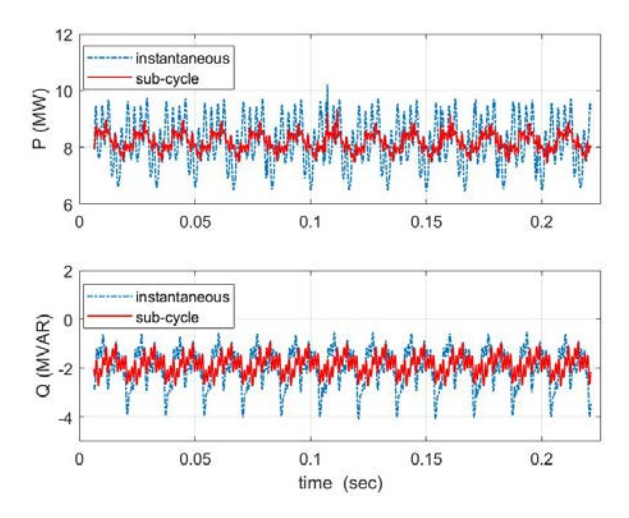


Fig. 3. Real-life steady-state example (steady-state-Hydro-Ottawa): real power (top), and reactive power (bottom). Dash-dot line used for instantaneous metrics, and solid line used for sub-cycle metrics (with $\xi = \frac{1}{4}$).

Similar results are obtained for transient waveforms that involve non-negligible harmonic distortion and/or unbalanced

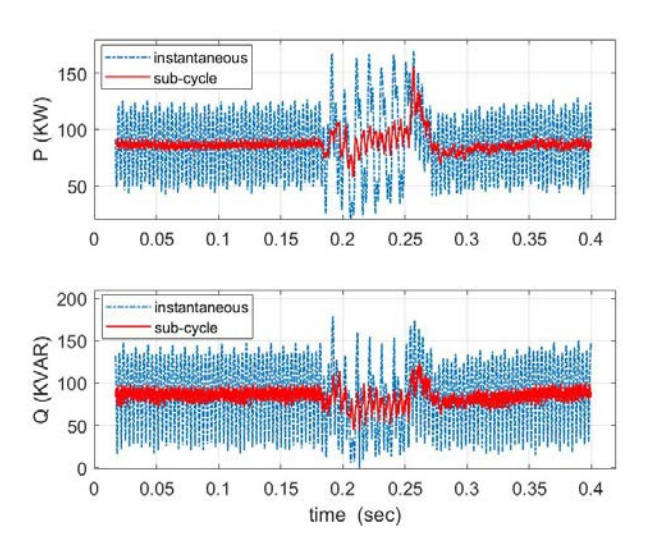


Fig. 4. Real-life transient example (paper-mill): real power (top), and reactive power (bottom). Dash-dot line used for instantaneous metrics, and solid line used for sub-cycle metrics (with $\xi = \frac{1}{4}$).

faults, such as the paper-mill example, the two transient-Hydro-Ottawa examples, the Brazilian-substation example, and the photo-voltaic system example, which are described in Secs. C, D, E and F of the Appendix, respectively. Figs. 4-8 exhibit a large fluctuating component in the instantaneous real and reactive power waveforms, which is generated by multiple harmonics and phase imbalance present in the current waveforms. In contrast, the sub-cycle metrics exhibit a relatively mild fluctuation in all of these examples.

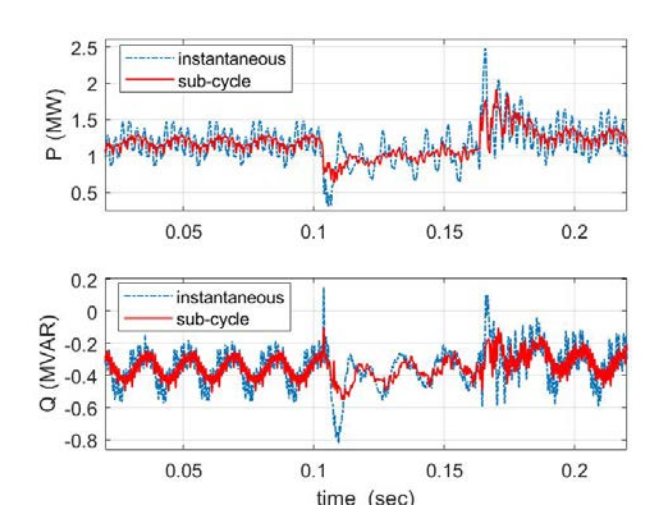


Fig. 5. Real-life transient example (transient-Hydro-Ottawa1): real power (top), and reactive power (bottom). Dash-dot line used for instantaneous metrics, and solid line used for sub-cycle metrics (with $\xi = \frac{1}{4}$).

We conclude that, in general, the 2-sample sub-cycle scheme offers a significant improvement in the quality of dynamic power metrics, as compared with the purely-instantaneous metrics of [6], [7], at a comparable computational cost (Table I). In particular, this means that the 2-sample sub-cycle $Q_{1/4}(t)$ can

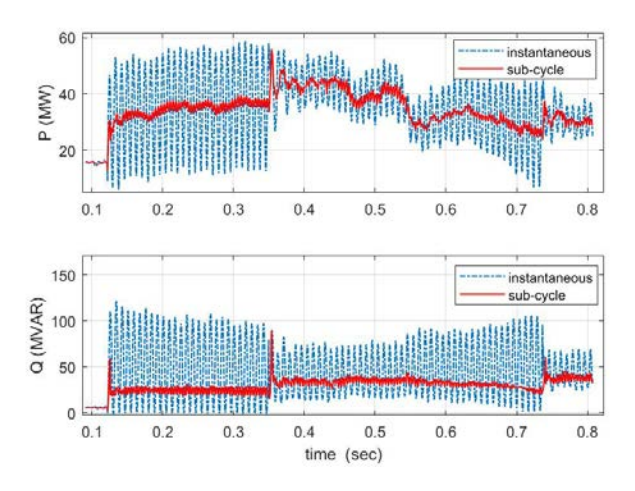


Fig. 6. Real-life transient example (transient-Hydro-Ottawa2): real power (top), and reactive power (bottom). Dash-dot line used for instantaneous metrics, and solid line used for sub-cycle metrics (with $\xi = \frac{1}{4}$).

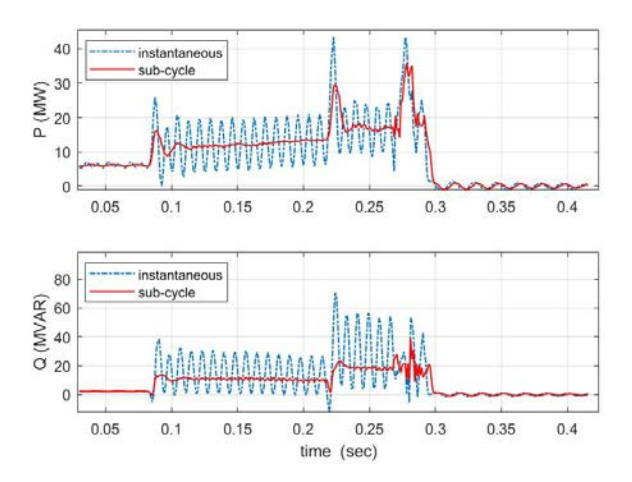


Fig. 7. Real-life transient example (Brazilian-substation-transient): real power (top), and reactive power (bottom). Dash-dot line used for instantaneous metrics, and solid line used for sub-cycle metrics (with $\xi = \frac{1}{4}$).

be used, without any cost increase, as a replacement for Akagi's q(t) in any algorithm that relies on the latter, including real-time control of industrial processes.

To be specific, we observe that evaluation of the instantaneous p(t) and q(t) in a 3-phase system requires 15 real multiplications and 9 real additions (Table I). In contrast, evaluation of the 2-sample sub-cycle P(t) and Q(t) for $\xi=\frac{1}{4}$ requires a comparable 14 real multiplications and 8 real additions, but produces much cleaner results with a significantly reduced fluctuating component (see Figs. 2-7).

In addition, the sub-cycle scheme provides additional power quality metrics that are not available in the purelyinstantaneous framework. For instance, the sub-cycle negativesequence components

$$P_{\xi}^{neg}(t) = \Re \left\{ \widehat{V}_{1,-}(t) \, \widehat{I}_{1,-}^{H}(t) \right\}$$

$$Q_{\xi}^{neg}(t) = \Im \left\{ \widehat{V}_{1,-}(t) \, \widehat{I}_{1,-}^{H}(t) \right\}$$
(7)

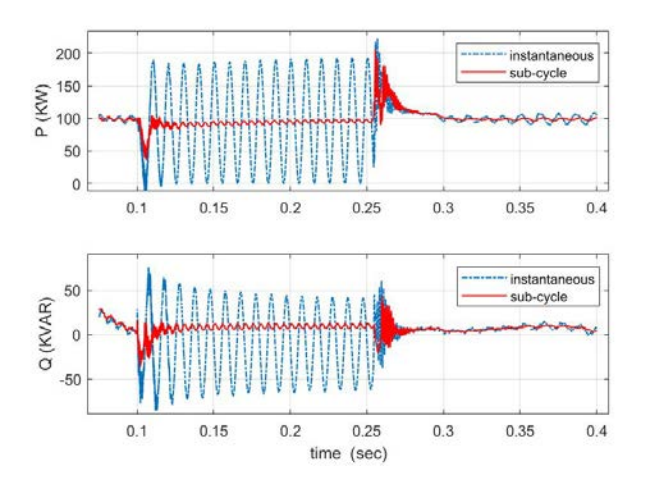


Fig. 8. Simulated fault example (PV system transient): real power (top), and reactive power (bottom). Dash-dot line used for instantaneous metrics, and solid line used for sub-cycle metrics (with $\xi = \frac{1}{4}$).

TABLE I. COST (PER TIME-INSTANT) COMPARISON OF PURELY-INSTANTANEOUS VS. 2-SAMPLE SUB-CYCLE

	Evaluating real power		Evaluating reactive power		Combined cost	
	mult.	add.	mult.	add.	mult.	add.
Purely-instantaneous	3	2	12	7	15	9
2-sample sub-cycle $(\xi=1/4)$	7	4	7	4	14	8

often provide accurate information about the duration and time of onset of a transient in 3-phase systems (similar expressions define the zero-sequence and positive-sequence components¹).

Transient timing information can also be extracted from the sub-cycle *N-metric*

$$N_{\xi}(t) \stackrel{\triangle}{=} \sqrt{S_{\xi}^{2}(t) - \left[P_{\xi}^{2}(t) + Q_{\xi}^{2}(t)\right]}$$
 (8)

which resembles the (full-cycle) Budeanu distortion power. Notice that, in the transient-Hydro-Ottawal example, the negative-sequence power $P_{\xi}^{neg}(t)$ (Fig. 9) is a more accurate timing indicator than the N-metric (Fig. 10).

In contrast, in the synthetic short-transient example² the accuracy of the $P_{\xi}^{neg}(t)$ metric is clearly inferior to that of the N-metric (see Figs. 11-12). We conclude that both metrics should be evaluated in scenarios involving transient phenomena.

¹The detailed construction of symmetrical sequence components for the 2-sample sub-cycle power metrics P(t) and Q(t) is described in [33].

²See Sec. G of the Appendix for details about this example.

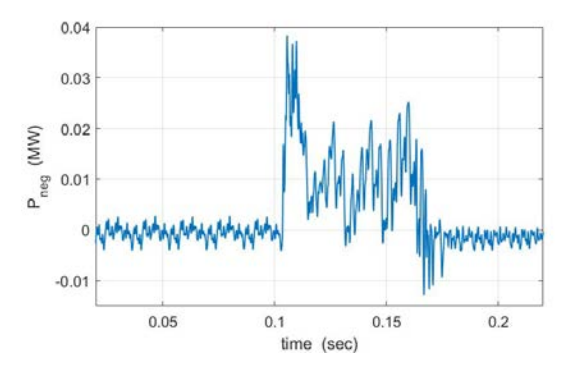


Fig. 9. Sub-cycle negative-sequence power (with $\xi=\frac{1}{4}$) in the transient-Hydro-Ottawal example.

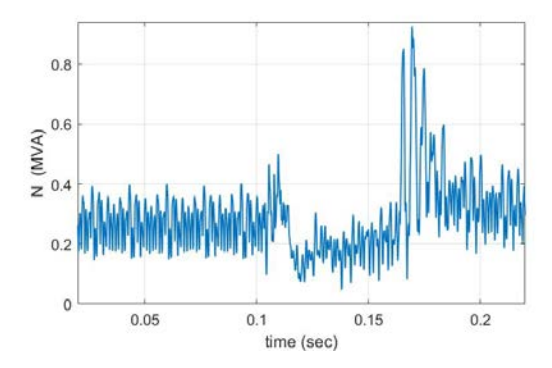


Fig. 10. Sub-cycle N-metric (with $\xi=\frac{1}{4}$) in the transient-Hydro-Ottawa1 example.

Sub-cycles schemes that rely on 4-samples or more can sometimes benefit from reducing the value of the control parameter ξ [29], [34]. However, our experience with the 2-sample sub-cycle scheme indicates that there is no advantage in using values other than $\xi=\frac{1}{4}$. In fact, as the value of ξ decreases, the performance of the 2-sample sub-cycle scheme can deteriorate quite dramatically, as demonstrated by Fig. 13 for the paper-mill case, with $\xi\approx\frac{1}{8}$. This should be compared with the even more extreme case of $\xi\to0$, shown in Fig. 14.

IV. DERIVATIVE-BASED REACTIVE POWER

The 2-sample dynamic sub-cycle phasor definition (3) can be approximated, for small values of the control parameter ξ , by the expression

$$\widehat{V}_1(t) e^{j\omega_0 t} \approx \frac{1}{\sqrt{2} (j2\pi\xi)} \left[(1 + j2\pi\xi) v(t) - v(t - \Delta) \right]$$

where $\Delta = \xi T$, and similarly for $\widehat{I}_1(t)$. Thus,

$$\begin{split} \widehat{V}_1(t) \, e^{j\omega_0 t} &\approx \frac{1}{\sqrt{2}} \Big[\, v(t) + \frac{v(t) - v(t - \Delta)}{j2\pi \xi} \, \Big] \\ &= \frac{1}{\sqrt{2}} \Big[\, v(t) - \frac{j}{\omega_0} \, \frac{v(t) - v(t - \Delta)}{\Delta} \, \Big] \end{split}$$

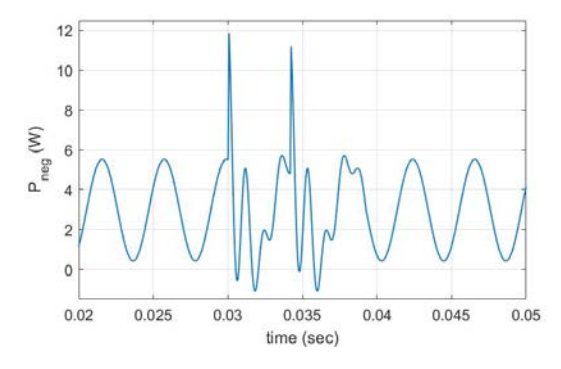


Fig. 11. Sub-cycle negative-sequence power (with $\xi = \frac{1}{4}$) in the synthetic-short-transient example

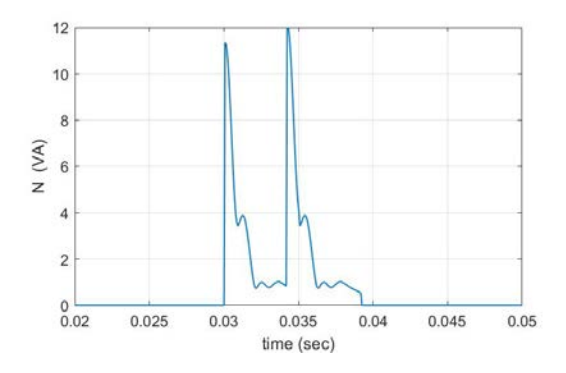


Fig. 12. Sub-cycle N-metric (with $\xi=\frac{1}{4}$) in the synthetic-short-transient example.

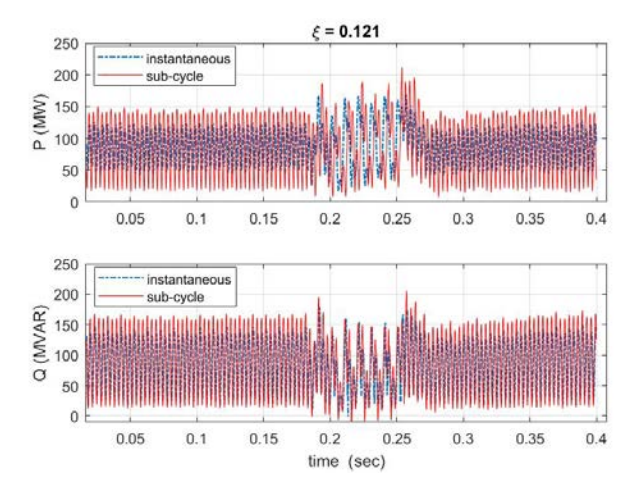


Fig. 13. Effect of reducing ξ in the real-life paper-mill example (with $\xi = 0.121$).

where we used the fact that $\omega_0 T=2\pi$. When $\xi\to 0$, this approximation converges to the exact expression

$$\left[\left. \widehat{V}_1(t) \right|_{\xi=0} \right] e^{j\omega_0 t} = \frac{1}{\sqrt{2}} \left[v(t) - j \left(\frac{1}{\omega_0} \frac{dv(t)}{dt} \right) \right]$$
(9a)

and, similarly,

$$\left[\widehat{I}_1(t) \Big|_{\xi=0} \right] e^{j\omega_0 t} = \frac{1}{\sqrt{2}} \left[i(t) - j \left(\frac{1}{\omega_0} \frac{di(t)}{dt} \right) \right]$$
 (9b)

which produces an explicit expression for the sub-cycle reactive power $Q_0(t)=\Im\{\widehat{V}_1(t)\,\widehat{I}_1^H(t)\}\Big|_{\varepsilon=0}$, viz.,

$$Q_0(t) \ = \ \frac{1}{2} \left[v(t) \left(\frac{1}{\omega_0} \, \frac{d}{dt} \, i(t) \right)^{\!\top} \!\! - \left(\frac{1}{\omega_0} \, \frac{d}{dt} \, v(t) \right) i^{\!\top} \! (t) \right] \ (10)$$

The same metric was introduced in [12], where it is denoted as $p_{react,2}(t)$, and also in [13], where it is denoted as $q^{\beta}(t)$. To be precise, $Q_0(t) \equiv q^{\beta}(t) = \frac{1}{\omega_0} \, p_{react,2}(t)$.

This derivative-based "instantaneous reactive power" metric has a number of useful theoretical properties [12], [13]:

- In a sinusoidal system $Q_0(t) = \Im\{V_1I_1^H\}$. In fact, this property holds for any value of ξ .
- Q₀(t) is positive for inductors, negative for capacitors, and zero for resistors.
- The cycle-averaged value of $Q_0(t)$ is related to energy storage in inductors and capacitors [13].
- $Q_0(t)$ is network-conservative, which means that its sum over all components in a network is zero. This allows for identification of sources and sinks of reactive power, which may lead to allocation of compensation requirements.

Notice, however, that any scheme for numerical evaluation of the voltage or current derivative requires at least two (closely-spaced) waveform samples, so that $Q_0(t)$ is not purely-instantaneous.

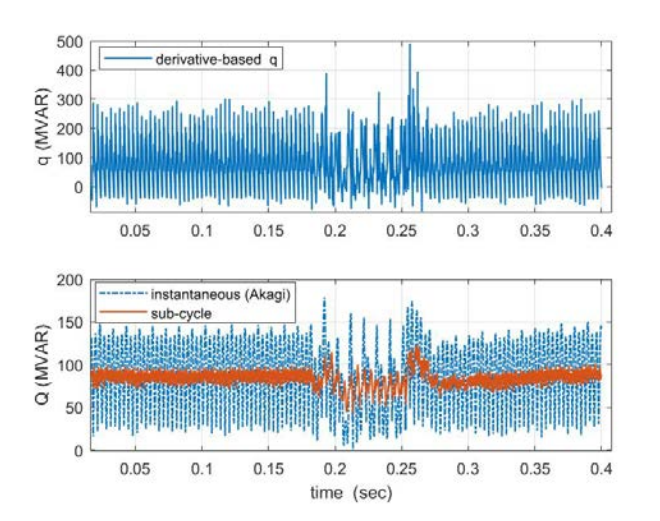


Fig. 14. Steady-state and transient fluctuation of dynamic reactive power (paper-mill example): derivative-based reactive power (top), sub-cycle (with $\xi = \frac{1}{4}$) and purely-instantaneous reactive power (bottom).

Furthermore, the reliance of (10) on current and voltage derivatives results in very high sensitivity to the presence of higher harmonics. To illustrate this effect we evaluate the 2-sample sub-cycle $Q_0(t)$ for the paper-mill data-set, and present it in Fig. 14: the top plot in this figure shows this metric, while the bottom plot is identical to the bottom plot of Fig. 4, which displays the 2-sample sub-cycle $Q_\xi(t)$ (for $\xi = \frac{1}{4}$) and the purely-instantaneous (Akagi) q(t). Notice that

the level of fluctuation of the derivative-based reactive power $Q_0(t) \equiv q^\beta(t) \equiv \frac{1}{\omega_0} \, p_{react,2}(t) \,\,$ is approximately 15 times higher than that of the sub-cycle $\,Q_{1/4}(t),\,$ and 3 times higher than that of the purely-instantaneous $\,q(t).\,$

Similar observations hold for the steady-state Hydro-Ottawa, the transient-Hydro-Ottawa1 and the wind-farm³ examples (Figs. 15-17): the level of fluctuation of the derivative-based reactive power $Q_0(t) \equiv q^\beta(t) \equiv \frac{1}{\omega_0} \, p_{react,2}(t)$ is significantly higher than that of the sub-cycle $Q_{1/4}(t)$.

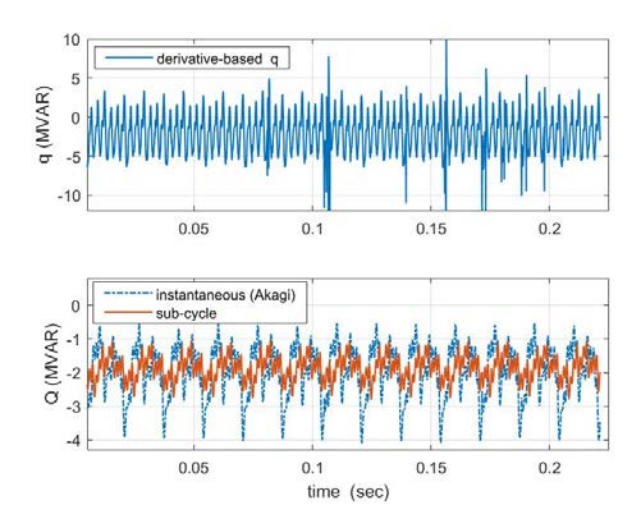


Fig. 15. Steady-state fluctuation of dynamic reactive power (steady-state-Hydro-Ottawa example): derivative-based reactive power (top), sub-cycle (with $\xi = \frac{1}{4}$) and purely-instantaneous reactive power (bottom).

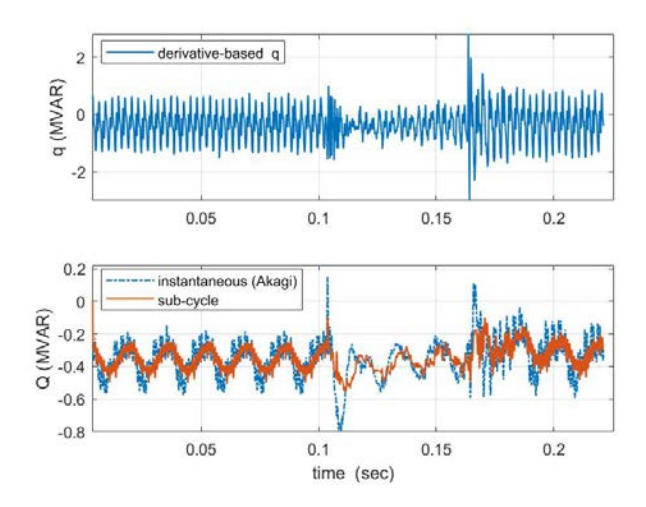


Fig. 16. Steady-state and transient fluctuation of dynamic reactive power (transient-Hydro-Ottawa1 example): derivative-based reactive power (top), sub-cycle (with $\xi=\frac{1}{4}$) and purely-instantaneous reactive power (bottom).

³See Sec. H of the Appendix for details about this example.

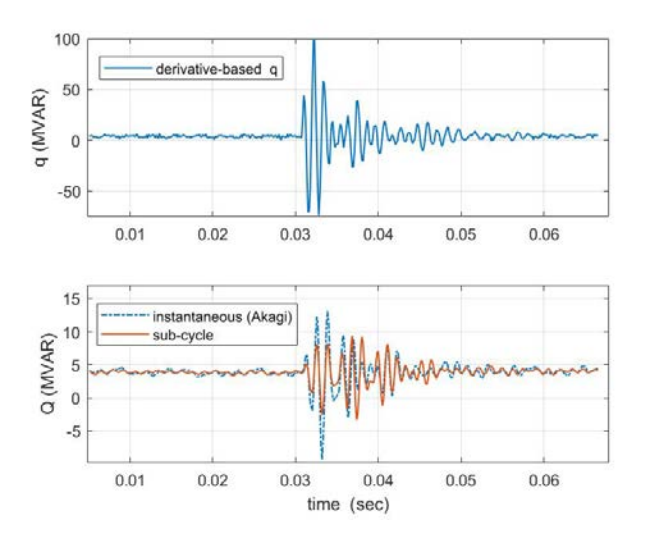


Fig. 17. Steady-state and transient fluctuation of dynamic reactive power (wind-farm example): derivative-based reactive power (top), sub-cycle (with $\xi = \frac{1}{4}$) and purely-instantaneous reactive power (bottom).

V. CONCLUDING REMARKS

We presented in this paper a scheme that uses only two samples of (polyphase) voltage and current to construct a number of dynamic power metrics, and compared its cost and performance with that of two alternative instantaneous reactive power metrics. We have shown that our 2-sample subcycle scheme (with $\xi=\frac{1}{4}$) has essentially the same low computational cost as the alternative metrics, which makes it particularly suitable for real-time industrial control applications. We used a number of industrial examples to demonstrate the superior performance of our 2-sample sub-cycle scheme, as compared with that of the purely-instantaneous q(t) of [6], and the "generalized instantaneous" reactive power metric $\frac{1}{\omega_0} p_{react,2}(t) \equiv q^\beta(t)$ of [12], [13], in both steady-state and in transient operation.

The 2-sample sub-cycle approach can be applied to any m-phase system, for any value of m, including the single-phase case. In contrast, the purely-instantaneous reactive power q(t) is defined only for three-phase systems with vanishing zero-sequence voltage and current. In addition, practical applications of the purely-instantaneous reactive power to compensation and active filter control require filtering to suppress the unwanted fluctuating component, which results in increased implementation cost and group-delay. In contrast, sub-cycle real and reactive power metrics can be used without further filtering, due to their low level of fluctuation in both steady-state and transient operation.

We have also explored the effects of reducing the value of the sub-cycle control parameter ξ . In particular, the sub-cycle reactive power $Q_0(t)$, obtained by setting $\xi \to 0$, is identical to the derivative-based instantaneous reactive power introduced in [12], [13]. We have demonstrated that this power metric exhibits a very high level of fluctuation, which severely limits its use in practical applications.

Our sub-cycle scheme offers several additional dynamic power metrics, which can be used to detect the onset of faults. In particular, the sub-cycle N-metric and the negative-sequence real-power component $P_\xi^{neg}(t)$ often provide accurate information about the duration and time-of-onset of a transient, and should both be evaluated in preparation for the possible occurrence of transients.

Finally, we should point out that the sub-cycle approach can, in general, be formulated to use any (even) number of polyphase voltage and current samples, with any number of phases. Increasing the number of waveform samples results in reduction of fluctuations, in both steady-state and transient operation, as well as improved accuracy of transient timing information. The most useful number of samples is M=4, as demonstrated in [28], [29], with only a minor improvement achieved by an increase to M=8 [34]. The attendant increase in computational cost is moderate: doubling the number of waveform samples used to calculate dynamic sub-cycle power metrics increases the cost by only a factor of three [28].

APPENDIX

A. RLC-load with higher harmonics

A three-phase steady-state system, driven by balanced fundamental and seventh harmonic voltages, with (rms) magnitudes $V_{1,rms} = \sqrt{1000}~V$ and $V_{7,rms} = 0.05~V_{1,rms}$. The unbalanced load consists of a resistor in phase a, an inductor in phase b, and a capacitor in phase c, each drawing a unit magnitude current at the fundamental harmonic. The sampling rate is 40 samples/cycle, and the fundamental frequency is $60~{\rm Hz}$.

B. Hydro-Ottawa steady-state

This real-world steady-state case was obtained from Hydro-Ottawa, the largest local distribution company in eastern Ontario, Canada. This data-set was recorded at 128 samples/cycle, on Jan. 7, 2017 at Hydro-Ottawa Site 100. The fundamental frequency is $60\,\mathrm{Hz}$.

C. Paper-mill transient [35]

This real-world transient case was extracted from a one year power-quality study (2004-2005) in the Mazandaran Wood and Paper Industries (MWPI), the largest paper manufacturer in Iran. The sampling rate is 140 samples/cycle, and the fundamental frequency is $50\,\mathrm{Hz}$.

D. Hydro-Ottawa transients

These two real-world transient cases were obtained from Hydro-Ottawa, the largest local distribution company in eastern Ontario, Canada. These data-sets were recorded at 128 samples/cycle, on June 26, 2017 at Hydro-Ottawa Site 10, and on Sept 26, 2017 at Hydro-Ottawa Site 1, respectively. The fundamental frequency is $60\,\mathrm{Hz}$.

E. Brazilian substation transient

This real-world transient case was obtained from the collection of data sets (comtrade files) recorded at a substation in Brazil named ETD BUTANTÃ which belongs to AES Eletropaulo utility. The sampling rate of the recorded waveforms is 16 samples/cycle, and the fundamental frequency is $60\,\mathrm{Hz}$.

F. PV system transient caused by a grid short-circuit [36]

This simulated transient case was generated by a model of a three-phase photovoltaic (PV) system, provided at: "https://ieee-dataport.org/open-access/study-three-phase-photovoltaic-systems-under-grid-faults", which allows simulations under various types of symmetrical and asymmetrical grid faults. This dataset corresponds to a line-to-line short in the grid power line. The fault response performance of the PV system takes into account ambient temperature and solar irradiance, grid codes, power control strategies, and grid conditions. The Simulink sampling rate of the waveforms is 20,000 samples/cycle, and the fundamental frequency is 50 Hz.

G. Synthetic short transient

A three-phase system, driven by balanced fundamental and fifth harmonic voltages, with equal unity magnitudes, and an injected 15-th harmonic transient. The load consists of three star-connected resistive-inductive impedances $Z_{1,k}=Z_{2,k}=Z_{3,k}=(1+j\,0.4\,k)\,\Omega$, where k (= 1 or 5) denotes the harmonic index. The sampling rate is 256 samples/cycle, and the fundamental frequency is 60 Hz. The corresponding steady-state voltage and current phasors are summarized in Table II.

TABLE II. SYNTHETIC SHORT TRANSIENT: STEADY-STATE VOLTAGE AND CURRENT PHASORS.

	a	b	c
V_1	$1 e^{j1.05}$	$0.8 e^{-j(-1.05+2\pi/3)}$	$0.8 e^{j(1.05+2\pi/3)}$
V_5	$0.8 e^{j6.28}$	$0.15 e^{-j(-6.28+2\pi/3)}$	$0.15 e^{j(6.28+2\pi/3)}$
I_1	$0.93 e^{j0.67}$	$0.93 e^{-j(-0.67+2\pi/3)}$	$0.93 e^{-j(0.67+2\pi/3)}$
I_5	$0.36 e^{j5.18}$	$0.36 e^{-j(-5.18+2\pi/3)}$	$0.36 e^{j(5.18+2\pi/3)}$

The injected transient (limited to the short time-interval $0.03 \sec < t < 0.035 \sec$), is given by the expressions

$$v_{trans}(t) = 5.5 e^{-t/0.0018} \cos (15 \omega_0 (t - 0.03))$$

 $i_{trans}(t) = 0.9 e^{-t/0.0018} \cos (15 \omega_0 (t - 0.03) - 1.4)$

where $\omega_0 = 120\pi$.

H. Wind-farm transient [37]

This real-world transient case was provided by the National Renewable Energy Laboratory (NREL), and collected from the Trent Mesa Wind Farm in Texas. A short transient in the current waveform is caused by switching in a bank of shunt capacitors. The sampling rate is 128 samples/cycle, and the fundamental frequency is $60\,\mathrm{Hz}$.

I. Online access to data sets

The data sets for all of our examples are available at: https://tufts.box.com/s/333wnbpt5xtwt7nzgo6x6o6jt956s73f

REFERENCES

- [1] D. Wiot, "A New Adaptive Transient Monitoring Scheme for Detection of Power System Events," *IEEE Trans. Power Delivery*, Vol. 19, No. 1, pp. 42 48, Jan. 2004.
- [2] R. Yadav, A.K. Pradhan and I. Kamwa, "Real-Time Multiple Event Detection and Classification in Power System Using Signal Energy Transformations," *IEEE Trans. Industrial Informatics*, Vol. 15, No. 3, pp. 1521 - 1531, March 2019.
- [3] O.P. Mahela, B. Khan, H.H. Alhelou and P. Siano, "Power Quality Assessment and Event Detection in Distribution Network With Wind Energy Penetration Using Stockwell Transform and Fuzzy Clustering," *IEEE Trans. Industrial Informatics*, Vol. 16, No. 11, pp. 6922 – 6932, Nov. 2020.
- [4] M. Simonov, G. Chicco and G. Zanetto, "Real-Time Event-Based Energy Metering," *IEEE Trans. Industrial Informatics*, Vol. 13, No. xx, pp. 2813 - 2823, Dec. 2017.
- [5] F. Zhang, H. Kodituwakku, J.W. Hines and J. Coble, "Multilayer Data-Driven Cyber-Attack Detection System for Industrial Control Systems Based on Network, System, and Process Data," *IEEE Trans. Industrial Informatics*, Vol. 15, No. 7, pp. 4362 - 4369, July 2019.
- [6] H. Akagi, Y. Kanazawa and A. Nabae, "Instantaneous Reactive Power Compensators Comprising Switching Devices Without Energy Storage Components," *IEEE Trans. Industry Applications*, Vol. 20, pp. 625-630, 1984.
- [7] H. Akagi, E.H. Watanabe, M. Aredes, Instantaneous Power Theory and Applications to Power Conditioning, Wiley, 2007.
- [8] F.Z. Peng and J.-S. Lai, "Generalized Instantaneous Reactive Power Theory for Three-phase Power Systems," *IEEE Trans. Instrumentation and Measurement*, Vol. 45, No. 1, pp. 293-297, Feb. 1996.
- [9] X. Dai, G. Liu and R. Gretsch, "Generalized theory of instantaneous reactive quantity for multiphase power system," *IEEE Trans. Power Delivery*, Vol. 19, No. 3, pp. 965-978, July 2004.
- [10] H. Lev-Ari and A.M. Stanković, "Instantaneous Power Quantities in Polyphase Systems – A Geometric Algebra Approach," *Energy Conversion Congress & Expo (ECCE)*, San Jose, CA, pp. 592-596, Sept. 2009
- [11] R. S. Herrera, P. Salmeron, J. R. Vazquez, S. P. Litran and A. Perez, "Generalized instantaneous reactive power theory in poly-phase power systems," 13th European Conference on Power Electronics and Applications, Barcelona, Spain, pp. 1-10, Sept. 2009.
- [12] J. Wyatt and M. Ilić, "Time-Domain Reactive Power Concepts for Nonlinear, Nonsinusoidal or Nonperiodic Network," *IEEE Intl. Symp. Circuits and Systems*, Vol. 1, No. 3, pp. 387-390, May 1990.
- [13] P. Tenti, P. Mattavelli, "A Time-domain Approach to Power Terms Definitions under Non-sinusoidal Conditions," 6th Int. Workshop on Power Definitions and Measurement under Non-Sinusoidal Conditions, Milan, Italy, 2003.
- [14] H. Kim, F. Blaabjerg, B. Bak-Nielsen and J. Choi, "Instantaneous Power Compensation in Three-Phase Systems by Using p-q-r Theory," *IEEE Trans. Power Electronics*, Vol. 17, No. 8, pp. 701-710, Sept. 2002.
- [15] M. Depenbrock, V. Staudt and H. Wrede, "Concerning Instantaneous Power Compensation in Three-Phase Systems by Using p-q-r Theory," *IEEE Trans. Power Electronics*, Vol. 19, No. 4, pp. 1151-1152, July 2004.
- [16] E.H. Watanabe, M. Aredes and H. Akagi, "The p-q Theory for Active Filter Control: Some Problems and Solutions," Revista Controle & Automação, Vol.15, No.1, pp. 78-84, Jan. 2004.

- [17] M. Popescu, A. Bitoleanu and V. Suru, "A DSP-Based Implementation of the p-q Theory in Active Power Filtering Under Nonideal Voltage Conditions," *IEEE Trans. Industrial Informatics*, Vol. 9, No. 2, pp. 880-889, May 2013.
- [18] M. Rivera, J. Rodriguez, J.R. Espinoza and H. Abu-Rub, "Instantaneous Reactive Power Minimization and Current Control for an Indirect Matrix Converter under a Distorted AC Supply," *IEEE Trans. Industrial Informatics*, Vol. 8, No. 3, pp. 482-490, Aug. 2012.
- [19] C.F. Garcia, M.E. Rivera, J.R. Rodriguez, P.W. Wheeler and R.S. Pena, "Predictive Current Control with Instantaneous Reactive Power Minimization for a Four-Leg Indirect Matrix Converter," *IEEE Trans. Industrial Electronics*, Vol. 64, No. 2, pp. 922-929, Feb. 2017.
- [20] N. Surasak and H. Fujita, "Control of a Three-Phase Diode Rectifier with an Instantaneous Reactive Power Compensator," 2020 IEEE Energy Conversion Congress and Exposition (ECCE), pp. 4579-4596.
- [21] L. Zhang and Y. Zhao, "Modeling and simulation of DC/AC converter for wind power flow optimization based on instantaneous reactive power theory," 2011 IEEE Power Engineering and Automation Conference, Vol. 1, pp. 183-186.
- [22] M. Marcu, F.G. Popescu, T. Niculescu, L. Pana and A.D. Handra, "Simulation of power active filter using instantaneous reactive power theory," 16th International Conference on Harmonics and Quality of Power (ICHQP), pp. 581-585, 2014.
- [23] H. Chen, A. Prasai and D. Divan, "A Modular Isolated Topology for Instantaneous Reactive Power Compensation," *IEEE Trans. Power Electronics*, Vol. 33, No. 2, pp. 975-986, Feb. 2018.
- [24] M. Eskandari, L. Li and M.H. Moradi, "Decentralized Optimal Servo Control System for Implementing Instantaneous Reactive Power Sharing in Microgrids," *IEEE Trans. Sustainable Energy*, Vol. 9, No. 2, pp. 525-537, Apr. 2018.
- [25] K. Takagi and H. Fujita, "A Three-Phase Grid-Connected Inverter Equipped With a Shunt Instantaneous Reactive Power Compensator," *IEEE Trans. Industry Applications*, Vol. 55, No. 4, pp. 3955-3966, July/Aug. 2019.
- [26] X. Kong, Y. Yuan, H. Huang and Y. Wang, "Overview of the instantaneous reactive power theory in three-phase systems," 5th International Conference on Electric Utility Deregulation and Restructuring and Power Technologies (DRPT), pp. 2331-2336, Nov. 2015.
- [27] L.S. Czarnecki, "Meta-theory of electric powers and present state of power theory of circuits with periodic voltages and currents," *Przeglad Elektrotechniczny*, Vol. 89, No. 6, pp. 26-31, 2013.
- [28] A. Ghanavati, H. Lev-Ari and A.M. Stanković, "A Sub-Cycle Approach to Dynamic Phasors with Application to Dynamic Power Quality Metrics," *IEEE Trans. Power Delivery*, Vol. 33, No. 5, pp. 2217-2225, Oct. 2018.
- [29] A. Ghanavati, H. Lev-Ari and A.M. Stanković, "Sub-Cycle Dynamic Phasors with Adjustable Transient Response," *IEEE Trans. Power Delivery*, Vol. 35, No. 4, pp. 1886-1894, Aug. 2020.
- [30] M. Iliovici, "Definition et mesure de la puissance et de l'energie reactives," Bull. Soc. Franc. Electr., no. 5, pp. 931-954, 1925.
- [31] A.G. Phadke and J.S. Thorp, *Synchronized Phasor Measurements and Their Applications*, 2nd edition, Springer, 2017.
- [32] Y. Bansal and R. Sodhi, "A Half-Cycle Fast Discrete Orthonormal S-Transform-Based Protection-Class μPMU," *IEEE Trans. Instrumentation and Measurement*, Vol. 69, No. 9, pp. 6934-6945, Sept. 2020.
- [33] H. Lev-Ari and A.M. Stanković, "A Sparse Sampling Approach to Dynamic Sub-Cycle Decomposition of Apparent Power in General Polyphase Networks," *Proceedings of the International School on Non-sinusoidal Currents and Compensation* (ISNCC 2015), Lagów, Poland, June, 2015.
- [34] A. Ghanavati, "A Sub-Cycle Approach to Dynamic Phasors with Application to Dynamic Power Quality Metrics," PhD Dissertation, Dept. of Electrical and Computer Engineering, Northeastern University, Boston, MA, May 2018.
- [35] M. Radmehr, Sh. Farhangi and A. Nasiri, "The Power of Paper: Effects

- of power quality distortions on electrical drives and transformer life in paper industries," *IEEE Industry Applications Magazine*, Vol. 13, No. 5, pp. 38-48, Sept.-Oct. 2007.
- [36] I. V. Banu and M. Istrate, "Study on three-phase photovoltaic systems under grid faults," *International Conference and Exposition on Electrical and Power Engineering (EPE)*, 2014, Iasi, pp. 1132-1137.
- [37] M. Islam, H.A. Mohammadpour, A. Ghaderi, C.W. Brice and Y.-J. Shin, "Time-Frequency-Based Instantaneous Power Components for Transient Disturbances According to IEEE Standard 1459," *IEEE Trans. Power Delivery*, Vol. 30, No. 3, pp. 1288 1297, June 2015.



Afsaneh Ghanavati (S'16, M'18) received the B.S. degree in electrical engineering from Shiraz University, Iran in 1998, and the M.S. and the Ph.D. in electrical engineering from Northeastern University, Boston, MA in 2012 and 2018 respectively. She is currently an assistant professor in the electrical and computer engineering program, School of Engineering at Wentworth Institute of Technology. Her present areas of interest include power systems, signal processing, dynamic phasors, power quality, and microgrid. She has been a member of the Eta

Kappa Nu, Engineering Honor Society and a member of IEEE Power & Energy Society (PES).



Hanoch Lev-Ari (M'84-SM'93-F'05) received the B.S., Summa Cum Laude, in 1971, and the M.S. in 1978, both in electrical engineering from the Technion, Israel Institute of Technology, Haifa, Israel; and the Ph.D. in electrical engineering from Stanford University, Stanford, CA, in 1984. He is currently a Professor with the Department of Electrical and Computer Engineering at Northeastern University. During 1994-1996 he was also the Director of the Communications and Digital Signal Processing (CDSP) Center at Northeastern University. Before

joining Northeastern, he was an Adjunct Research Professor of Electrical Engineering with the Naval Postgraduate School, Monterey, CA and a Senior Research Associate with the Information Systems Laboratory at Stanford University. He served as an Associate Editor of Circuits, Systems and Signal Processing, and of the IEEE Transactions on Circuits and Systems I, and is a member of SIAM.



Aleksandar M. Stanković (F'05) obtained his Ph.D. degree from Massachusetts Institute of Technology in 1993 in electrical engineering. He presently serves as A.H. Howell Professor at Tufts University; he was with Northeastern University, Boston 1993-2010. He is a Fellow of IEEE and serves as an Associate Editor for *Annual Reviews in Control*. He has previously served the IEEE Transactions on Smart Grid, on Power Systems and on Control System Technology in the same capacity. He has held visiting positions at the United Technologies Research Center (sabbati-

cals in 2000 and 2007) and at L'Universite de Paris-Sud and Supelec (in 2004). He is a co-editor of book series on Power Electronics and Power Systems for Springer.